UDC 548.73:541.49:546.48

ORGANIC-INORGANIC HYBRID PEROVSKITE $(C_6H_5(CH_2)_2NH_3)_2CdCl_4$: SYNTHESIS, STRUCTURAL AND THERMAL PROPERTIES

S. Kassou[1], A. Kaiba[2], P. Guionneau[3], A. Belaaraj[1]

[1]*Laboratoire de Physique des Matériaux et Modélisation des Systèmes, CNRST-URAC08, Faculté des Sciences, Université Moulay Ismail, B.P. 11201, Zitoune, 50000 Meknès, Maroc*
 E-mail: a.belaaraj@fs-umi.ac.ma
[2]*Physics Department, College of Sciences and Humanity, Prince Sattam bin Abdulaziz University, P.O. Box 83, Al-Kharj11942, Saudi Arabia*
[3]*CNRS, Université Bordeaux, ICMCB, UPR 9048, F-33600 Pessac, France*

The present research work reports the study on crystal structure, vibrational spectroscopy and thermal analysis of organic-inorganic hybrid compound $(C_6H_5(CH_2)_2NH_3)_2CdCl_4$. Single crystals of bis(phenethylammonium)tetrachlorocadmate $(C_6H_5(CH_2)_2NH_3)_2CdCl_4$ (PEA—Cd) were obtained by diffusion at room temperature. This compound crystallizes in the orthorhombic space group $C2cb$ with unit cell parameters $a = 7.4444(2)$ Å, $b = 38.8965(3)$ Å, $c = 7.3737(2)$ Å and $Z = 4$. Single crystal structure has been solved and refined to $R = 0.036$ and $wR = 0.092$. The structure consists of an extended $[CdCl_4]^{2-}$ network and two $[C_6H_5(CH_2)_2NH_3]^+$ cations to form a two-dimensional perovskite system. The infrared (IR) spectrum of the title compound was recorded at room temperature. Differential scanning calorimetry (DSC) was used to investigate the phase transition; this compound exhibits a reversible single solid-solid phase transition.

INTRODUCTION

Bis(phenethylammonium) tetrachlorocadmate (PEA—Cd) belongs to a large family of organic-inorganic hybrid perovskite-like systems with a general formula $((R—NH_3)_2MX_4$ (where R = Organic part, M = Transition metal and X = Halogen), which have been widely investigated in the last few years because of the enormous variety and their potential technological applications [1]. This family presents the synergy between organic and inorganic entities. The first one has specific properties like high fluorescence efficiency, large polarizability, plastic mechanical properties and structural diversity. The second one is characterized by a wide range of electronic properties, magnetic, dielectric transitions, substantial hardness, and thermal stability. The inorganic moieties consist of infinite sheets made up of corner-sharing octahedra MX_6 (M = Mn, Cu, Mg, Cd, Fe). On the other hand, isolated MX_4 tetrahedra have been found for M = Co, Zn. The organic moieties comprise *n*-alkylammonium groups linked to the inorganic layers. The voids between the octahedra are occupied by the terminal NH_3 head; they form N—H…X bonds with the halogen atoms [2—4]. The interlayer cohesion is maintained by hydrogen bonds, van der Waals or π—π stacking interactions. These kinds of systems can be used for thermal energy storage [5—9]. This work is the continuation of the studies on this type of materials [10]. M. Groh et al. have synthesized another phase of the title compound (ortho-

rhombic space group *Pcab*, $a = 38.8965(2)$ Å, $b = 7.4340(10)$ Å, $c = 7.3671(10)$ Å and $Z = 4$) [11]. In this paper, we have synthesized a new phase of PEA—Cd. The structural, spectroscopic and thermal properties were characterized by X-ray diffraction (XRD), infrared spectroscopy (FT-IR) and differential scanning calorimetry (DSC).

EXPERIMENTAL

Crystal growth. All chemicals of reagent quality were purchased from Aldrich. The single crystal of organic-inorganic hybrid $(C_6H_5(CH_2)_2NH_3)_2CdCl_4$ was grown from an ethanol/water solution at room temperature. The title compound was prepared by dissolving 0.25 g of phenethylamine in 5 ml of water/ethanol (1:1 ratio) followed by addition of 1.8 ml of HCl (37 %). A weigh of 0.471 g of $CdCl_2$ was dissolved in 3 ml of water. The solutions were combined and kept at room temperature in a glass tube to afford white plate-like crystals after few weeks.

Characterization of the PEA—Cd crystal. FT-IR spectra (KBr pellets) were recorded on a Jasco FT/IR 4100 spectrometer in the range 4000—400 cm^{-1}. Powder X-ray diffraction patterns were recorded with a Shimadzu X-ray Diffractometer (XRD) using graphite monochromated CuK_α radiation. The purity and crystallinity of the sample were examined using powder X-ray diffraction. XRD pattern of the title material and the pattern simulated from its structure are shown in Fig. 1; it is evident that the purity is high. The differential scanning calorimetry (DSC) measurements were performed using a DSC 131Evo instrument. The experiment was carried out from room temperature up to 600 K with ramp rate 5 °/min under nitrogen atmosphere. Those measurements have been repeated three times on the same sample.

A crystal of size 0.5×0.5×0.03 mm was selected under an optical microscope and used for single-crystal X-ray diffraction. The measurements were performed on a Nonius Kappa CCD with MoK_α radiation with graphite monochromator. Data collection was made at room temperature using Φ, Ω scan mode, the crystal to detector distance was 35.30 mm, further details are given in Table 1. The structure was solved by SIR97 [12] and the refinement of atomic parameters based on full-matrix least squares on F^2 was performed using SHELX97 [13]. All non-hydrogen atoms were refined anisotropically and the hydrogen atoms were located in idealized positions. All above programs were used within the WINGX package [14]. The molecular graphics was prepared using the DAIMOND program [15].
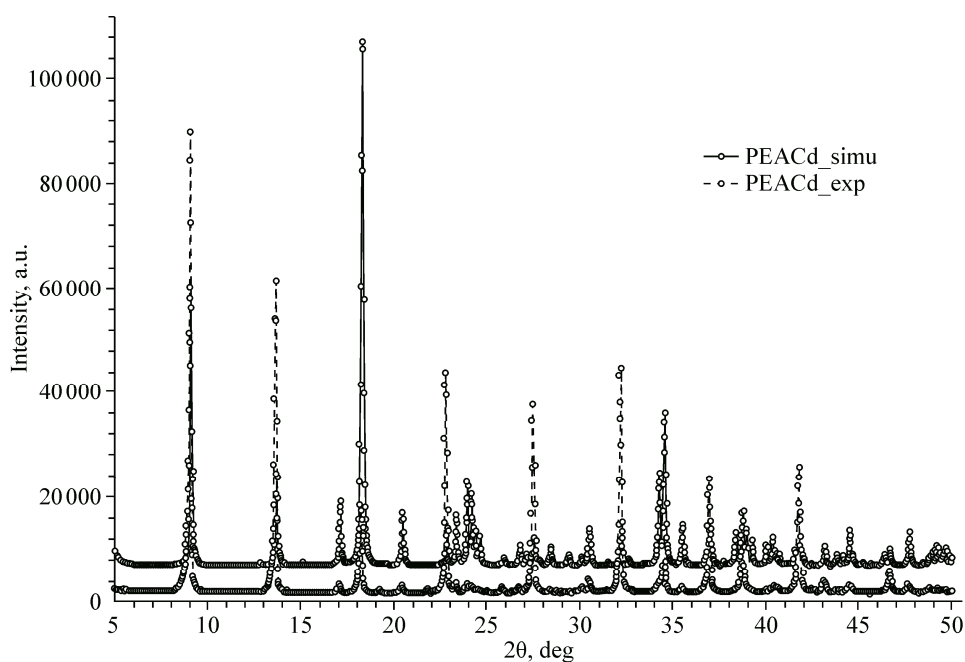

Fig. 1. Experimental and simulated X-ray diffraction patterns of PEA—Cd

T a b l e   1

Crystallographic data and structure refinement of PEA—Cd

Empirical formula	$C_{16}H_{24}CdC_{14}N_2$
Formula weight	498.57
Temperature, K	293(2)
Wavelength, Å	0.71073
Crystal system	Orthorhombic
Space group	*C2cb*
Unit cell dimensions *a*, *b*, *c*, Å	7.4444(2), 38.8965(3), 7.3737(2)
Volume, Å^3	2135.14(5)
Z	4
Density (calculated), mg/m^3	1.551
Absorption coefficient, mm^{-1}	1.523
Crystal size, mm	0.5×0.5×0.03
θ range, deg.	3.14—26.36
Range of *h*, *k*, *l*	−9→9, −47→48, −9→9
Reflections collected / independent	2087 / 2087
Data / restraints / parameters	2087 / 48 / 87
Goodness-of-fit on F^2	1.152
Final *R* indices [$I > 2\sigma(I)$]	$R_1 = 0.0363$, $wR_2 = 0.0925$
Largest diff. peak and hole, e/Å^3	0.666 and −0.597

The crystallographic data for the structure described in this paper was deposited to the Cambridge Crystallographic Data Center, deposition number CCDC 964405.

RESULTS AND DISCUSSION

FT-IR spectral analysis. The assignment of the internal modes of this compound is based on the comparison to homologous compound [16—25]. The infrared spectrum (Fig. 2) shows that the frequency of the stretching mode (ν_s; 3105 cm^{-1}, ν_a; 3166 cm^{-1}) of NH_3^+ in PEA—Cd compound is lower compared to NH$_2$ frequency (ν_s; 3285 cm^{-1}, ν_a; 3370 cm^{-1}) in phenethylamine ($C_6H_5(CH_2)_2NH_2$). This can be ascribed to the changing of NH$_2$ chemical environment as a result of N—H…Cl hydrogen bond
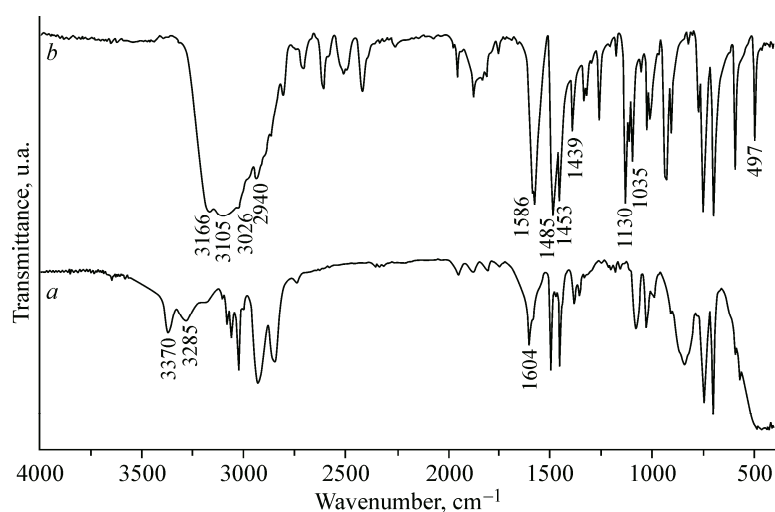

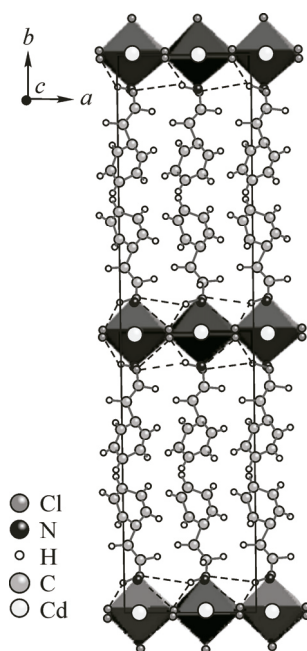*Fig. 2.* Infrared spectrum of: phenethylamine (*a*), PEA—Cd (*b*)

Fig. 3. Overall view of the crystal packing. The hydrogen
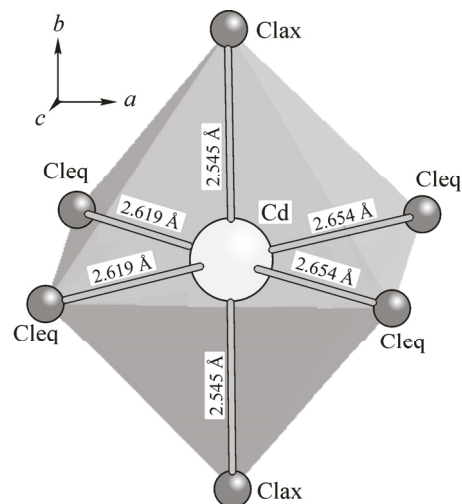bonds network is represented by light blue dotted lines

Fig. 4. View along c axis of the $CdCl_6$
octahedron

formation [26]. The band observed at 2800—3000 cm^{-1} range is assigned to the symmetric/asymmetric stretching vibration of (—CH_2—). The symmetric deformation band of the NH_3^+ entity is observed at 1586 cm^{-1}. The band located at 1485 cm^{-1} is due to the (—CH_2—) scissor mode, while the bands at 1453 and 1389 cm^{-1} are assigned to asymmetric and symmetric deformation modes of (—CH_2—), respectively. The bands at 1130 and 1095 cm^{-1} are associated to aromatic in plane (—CH—) bending vibration and (—C—N—) stretching vibration, respectively. The band at 930 cm^{-1} is assigned to (—CH_2—) wagging vibration. The aromatic (=CH) deformation modes in and out of ring plane are observed in 750—950 cm^{-1} range. The aromatic ring deformation bands in and out of ring plane appear at 697 and 594 cm^{-1} respectively. The band at 746 cm^{-1} is attributed to (—CH_2—) rocking vibration, and the peak of NCC angle deformation in twisted conformation is located at 497 cm^{-1}.

Crystal structure description. Crystallographic data, details of the measurements (room temperature) and refinement are summarized in Table. 1. The compound crystallizes in the orthorhombic system with $C2cb$ space group, $a = 7.4444(2)$ Å, $b = 38.8965(3)$ Å, $c = 7.3737(2)$ Å and $Z = 4$. The asymmetric unit cell consists of one $[CdCl_4]^{2-}$ anion and two $[C_6H_5(CH_2)_2NH_3]^+$ cations. The structure can be described by alternation of organic and inorganic layers stacked along the a axis (Fig. 3). Indeed, within the inorganic sheet, the nearest distance between neighboring metallic sites connected by the Cd—Cl—Cd bridge is $d_{intra} = 5.2390$ Å, while the distance between two adjacent inorganic layers is $d_{inter} = 19.4482$ Å. The large value of the ratio $d_{inter}/d_{intra} = 3.712$ gives the layered structure for this compound. The inorganic layers consist of $CdCl_6$ octahedra in which two shorter Cd—Cl bonds are nearly perpendicular to the layer (Cd(1)—Cl(1)$_{ax}$ = 2.545 Å), and four longer bonds are Cd(1)—Cl(2)$_{eq1}$ = 2.654 Å. The Cd—Cl—Cd bridges are symmetric though the bridging angle is not linear and equals 166.7°. The coordination geometry around the Cd atoms shows slight axial compression of the octahedral geometry, with the bridging Cd—Cl_{eq} distances longer than the axial distances Cd—Cl_{ax} (Fig. 4).

In order to structurally characterize the cadmium site and estimate the distortion, we use here the value of the twelve Cl—Cd—Cl angles to estimate the Σ parameter [26], that is the sum of the deviations from 90° of the twelve angles in the coordination sphere. The value of Σ is about 10.7° for the title compound, a large deviation from the ideal octahedral geometry is observed. This coordination
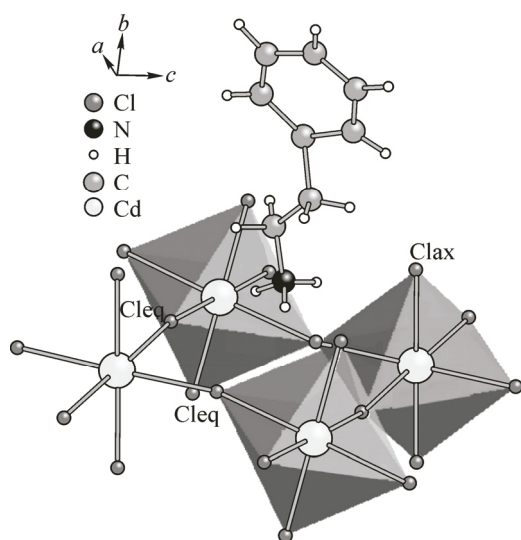
Fig. 5. Scheme of hydrogen-bonding interactions between phenethylammonium and inorganic layers
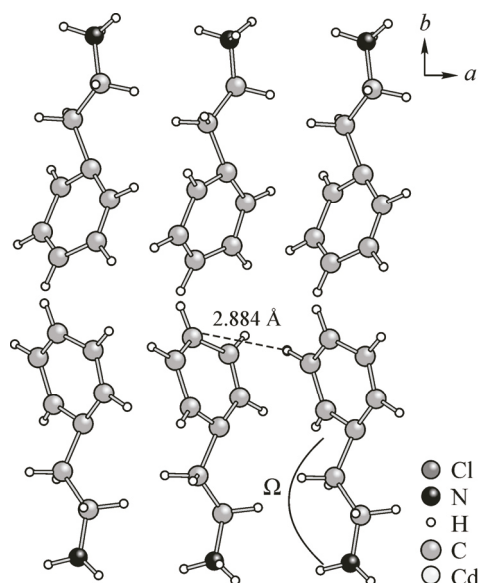

Fig. 6. Scheme of short contacts between neighboring organic species

geometry can be compared to analogous compounds. Indeed, for manganese the coordination geometry shows no axial compression of octahedral geometry, $\Sigma = 7.0°$ [27]. The coordination geometry around lead as the metal center and bromine as the halogen ligand shows high distortion coefficient ($\Sigma = 37.5°$) [28]. The compounds with copper(II) show strong Jahn—Teller distortion, each of Cu(II) atoms forms four short Cu—X (X = Cl, Br) bonds in a planar arrangement and two longer semi-coordinate Cu—X bonds [29—31].

The organic moieties $[C_6H_5(CH_2)_2NH_3]^+$ are aligned nearly perpendicular to the inorganic layer *via* N—H…Cl hydrogen bonding. Based on the bond lengths and angles of the N—H…Cl bonds [32], the hydrogen bonds were classified as two strong and two weak bonds. The two strong hydrogen bonds are formed with chlorines Cl_{ax} and Cl_{eq} and a bifurcated weak hydrogen bond is formed with two chlorines Cl_{ax} and Cl_{eq} (Fig. 5). The $CdCl_6$ octahedron is slightly tilted by ~7.25° as a result of hydrogen bonding.

The crystal packing cohesion is also built on π—π stacking interactions between neighboring phenyl ring moieties. The distance d (5.12 Å) between centroids of the corresponding rings and the two angles α (71.5°) and α_0 (6.4°) between the normal of each mean plane through these rings and the centroid-centroid axis show that the rings are close to being perpendicular and involve a weak π-stacking [33]. In fact, the difference between α and α_0 is large (65.1°), also d distances are increased. There is a weak π-stacking effect. Moreover, the cohesion between organic moieties is supported by C—H…C interaction of 2.884 Å (Fig. 6). The value of N—C—C—C torsion angle (Ω) is about 166.5°. We believe that the twisted conformation is responsible for the phase transition shown by the DSC analysis.

Thermal analysis (DSC). The thermal study was carried out by heat flow measurement using differential scanning calorimetry. The compound decomposition temperature is about to 623 K. Fig. 7 shows heat flow between room temperature and decomposition;
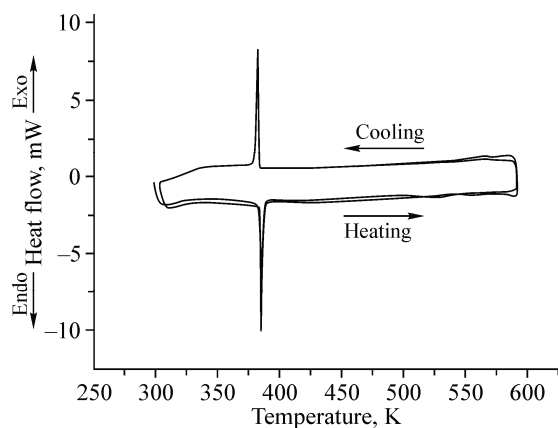

Fig. 7. Differential scanning calorimetry measurements of PEA—Cd

one phase transition appears at 385 K. This transition shows a peak caused by latent heat characteristic of the first-order phase transition. The heating and cooling curves provide evidence for hysteresis, which characterizes a first-order phase transition. Indeed, the endothermic peak at 385 K is accompanied by an enthalpy $\Delta H = 7.48$ kJ/mol during heating and the exothermic peak at 382 K is accompanied by an enthalpy $\Delta H = -7.67$ kJ/mol during cooling. The hysteresis width is about 3 K and this phase transition is perfectly reversible. This transition originates from order-disorder transition of the alkyl ammonium ions [34—35].

CONCLUSIONS

The organic-inorganic hybrid PEA—Cd has been synthesized successfully by diffusion method. The single crystal X-ray diffraction investigation of the title compound at room temperature confirms the formation of the 2D layered perovskite system. The infrared spectrum shows NCC deformation mode. This type of the vibrational mode plays crucial role in the thermal phase transition. A reversible transition has been shown by differential scanning calorimetry measurements.

REFERENCES

1. *Mitzi D.* // Prog. Inorg. Chem. – 2007. – **48**. – P. 1 – 121.
2. *Kind R., Plesko S., Arend H. et al.* // J. Chem. Phys. – 1979. – **71**. – P. 2118 – 2130.
3. *Kitazawa N., Aono M., Watanabe Y.* // J. Phys. Chem. Solids. – 2011. – **72**, N 12. – P. 1467 – 1471.
4. *Guo L., Liu H., Dai Y. et al.* // J. Phys. Chem. Solids. – 2007. – **68**, N 9. – P. 1663 – 1673.
5. *Courseille C., Chanh N., Maris T. et al.* // Phys. Status Solidi A. – 1994. – **143**, N 2. – P. 203 – 214.
6. *Vishwakarma A.K., Ghalsasi P.S., Navamoney A. et al.* // Polyhedron. – 2011. – **30**, N 9. – P. 1565 – 1570.
7. *Cheng Z., Gao B., Pang M. et al.* // Chem Mater. – 2003. – **15**, N 25. – P. 4705 – 4708.
8. *Zheng Y.Y., Wu G., Deng M. et al.* // Thin Solid Films. – 2006. – **514**, N 1. – P. 127 – 131.
9. *Busico V., Corradini P., Vacatello M., Fittipaldi F., Nicolais L.-C.* In: Thermal Storage of Solar Energy / Ed. C. den Ouden. – Netherlands: Springer, 1981. – P. 309 – 324.
10. *Billing D., Lemmerer A.* // Acta Crystallogr. B. – 2007. – **63**, N 5. – P. 735 – 747.
11. *Groh M., Spengler R., Burzlaff H. et al.* // Acta Crystallogr. C. – 1997. – **53**, N 9. – P. 1199 – 1201.
12. *Altomare A., Burla M., Camalli M. et al.* // J. Appl. Crystallogr. – 1999. – **32**, N 1. – P. 115 – 119.
13. *Sheldrich G.M.* SHELX-97, release 97-2. – Germany: University of Goettingen, 1998.
14. *Farrugia L.* // J. Appl. Crystallogr. – 1999. – **32**, N 4. – P. 837 – 838.
15. *Brandenburg K.* DIAMOND-3.1. – Bonn, Germany: Crystal Impact GbR, 1997.
16. *Chaabane I., Hlel F., Guidara K.* // PMC Physics B. – 2008. – **1**, N 11. – P. 1 – 19.
17. *Guan J., Tang Z., Guloy A.M.* // Chem. Commun. – 1999. – **18**. – P. 1833 – 1834.
18. *Ivanova B.B., Arnaudov M.G., Mayer-Figge H.* // Polyhedron. – 2005. – **24**. – P. 1624 – 1630.
19. *Venkataraman N.V., Bhagyalakshmi S., Vasudevan S. et al.* // Phys. Chem. Chem. Phys. – 2004. – **4**. – P. 4533 – 4538.
20. *Kefi R., Zeller M., Lefebvre F. et al.* // Int. J. Inorg. Chem. – 2011. – **2011**. – P. 1 – 7.
21. *Socrates G.* Infrared Characteristic Group Frequencies: Tables and Chart. – UK: John Wiley & Sons, 1994.
22. *Elmebrouki K., Khechoubi E., Kaiba A. et al.* // J. Asian Sci. Res. – 2013. – **3**, N 5. – P. 454 – 461.
23. *Xiao Z.L., Chen H.Z., Shi M.M. et al.* // Mater. Sci. Eng. B. – 2005. – **117**, N 3. – P. 313 – 316.
24. *Staśkiewicz B., Baran J., Czapla Z.* // J. Phys. Chem. Solids. – 2013. – **74**. – P. 1848 – 1858.
25. *Cheng Z., Wang Z., Xing R. et al.* // Chem. Phys. Lett. – 2003. – **376**, N 3. – P. 481 – 486.
26. *Guionneau P., Marchivie M., Bravic G. et al.* // Top. Curr. Chem. – 2004. – **234**. – P. 97 – 128.
27. *Park S.H., Oh I.H., Park Y. et al.* // Dalton Trans. – 2012. – **41**. – P. 1237 – 1242.
28. *Shibuya K., Koshimizu M., Nishikido F. et al.* // Acta Crystallogr. E. – 2009. – **65**, N 11. – P. 1323 – 1324.
29. *Polyakov A.O., Arkenbout A.H., Baas J. et al.* // Chem. Mater. – 2011. – **24**, N 1. – P. 133 – 139.
30. *Billing D., Lemmerer A.* // CrystEngComm. – 2006. – **8**, N 9. – P. 686 – 695.
31. *Willet R.* // Acta Crystallogr. C. – 1990. – **46**. – P. 565 – 568.
32. *Steiner T.* // Angew. Chem. Int. Ed. Eng. – 2002. – **141**, N 1. – P. 48 – 76.
33. *Janiak C.* // J. Chem. Soc., Dalton Trans. – 2000. – **12**. – P. 3885 – 3896.
34. *Yoshinari T., Nanba T., Shimanuki S. et al.* // J. Phys. Soc. Jpn. – 1992. – **61**. – P. 2224 – 2226.
35. *Mitzi D.* // Chem. Mater. – 1996. – **8**, N 3. – P. 791 – 800.